

Many-Body Perturbation Theory Applied to Open-Shell Atoms*

HUGH P. KELLY†

Institute for Radiation Physics and Aerodynamics, University of California, San Diego, La Jolla, California

(Received 9 September 1965)

It is shown how many-body perturbation theory may be applied to the problem of correcting Hartree-Fock energies and wave functions for the degenerate ground states of open-shell atoms. The choice of an appropriate potential for the calculation of the single-particle states of the perturbation expansion is discussed in detail. As an example of these methods, the correlation energies among all pairs of electrons in the neutral oxygen atom are calculated for excitations into $1=0, 1, 2,$ and 3 states. The total calculated pair correlation energy is -0.274 atomic units (a.u.) as compared with the total correlation energy -0.258 a.u. which is deduced from experiment. The correlation energy among $2p-2p$ electron pairs is -0.0906 a.u.; among $2s-2p$ pairs, -0.1004 a.u.; $2s-2s$, -0.0150 a.u.; $1s-2p$, -0.014996 a.u.; $1s-2s$, -0.00629 a.u.; $1s-1s$, -0.0438 a.u. There is also a contribution -0.0028 a.u. which corrects for the use of a restricted Hartree-Fock solution.

I. INTRODUCTION

THE many-body perturbation theory developed by Brueckner¹ and Goldstone² has been successfully used in calculations of nuclear structure³ and of correlations in the high-density electron gas.⁴ In addition, this theory has recently been applied to atoms to obtain corrections to Hartree-Fock (HF) solutions and to calculate other atomic properties.^{5,6} Results have been obtained for the correlation energies among the different electron pairs in the neutral beryllium atom which are in good agreement with experiment.⁵ Calculations have also been made of dipole and quadrupole polarizabilities and shielding factors and of transition probabilities, all for neutral beryllium.⁶

Although the many-body perturbation theory is quite applicable to atoms with few electrons, its greatest value may be in calculations for atoms with many electrons. The purpose of this paper is to consider the application of many-body perturbation theory to atoms which are considerably more complicated than those of beryllium. As an example, the correlations among all electron pairs of the neutral oxygen atom are studied in detail. Oxygen is an eight-electron atom with a non-spherically symmetric ground state.

The perturbation theory of Brueckner and Goldstone is reviewed in Sec. II. In Sec. III the choice of an appropriate unperturbed ground-state wave function is considered and it is shown how the perturbation theory may be applied in cases where the electrons do not form

closed shells. The selection of the potential to be used in calculating the single-particle states is discussed in Sec. IV. In Sec. V the correlation energies among all pairs of electrons in oxygen are calculated. Section VI contains the discussion and conclusions.

I. REVIEW OF PERTURBATION THEORY

The total Hamiltonian H for a system of N identical fermions interacting through two-body potentials v_{ij} is given by

$$H = \sum_{i=1}^N T_i + \sum_{i<j}^N v_{ij}, \quad (1)$$

where T_i is the sum of the kinetic-energy operator for the i th particle and all one-body potentials for the i th particle. For atoms,

$$T_i = -\nabla_i^2/2 - Z/r_i, \quad (2)$$

where the term $-Z/r_i$ is the interaction of the i th electron with the nucleus of charge Z . Atomic units are used throughout this paper.⁷ The correct ground-state wave function Ψ_0 satisfies the eigenvalue equation

$$H\Psi_0 = E\Psi_0, \quad (3)$$

where E is the exact nonrelativistic ground-state energy.

A great simplification is achieved by approximating the effect of the N interacting particles by a single-particle potential V . The Hamiltonian H is then replaced by

$$H_0 = \sum_{i=1}^N (T_i + V_i), \quad (4)$$

and Ψ_0 is approximated by Φ_0 which satisfies the eigenvalue equation

$$H_0\Phi_0 = E_0\Phi_0. \quad (5)$$

The correct ground-state energy E is now approximated by E_0 . The potential V must be Hermitian so that the

⁷D. R. Hartree, *The Calculation of Atomic Structures* (John Wiley & Sons, Inc., New York, 1957), p. 5.

* This research was supported by the Advanced Research Projects Agency (Project DEFENDER) and was monitored by the U. S. Army Research Office—Durham under Contract DA-31-124-ARO-D-257.

† Present address: Physics Department, University of Virginia, Charlottesville, Virginia.

¹K. A. Brueckner, *Phys. Rev.* **97**, 1353 (1955); **100**, 36 (1955); *The Many-Body Problem* (John Wiley & Sons, Inc., New York, 1959).

²J. Goldstone, *Proc. Roy. Soc. (London)* **A239**, 267 (1957).

³K. A. Brueckner and J. L. Gammel, *Phys. Rev.* **109**, 1023 (1958); K. A. Brueckner and K. S. Masterson, Jr., *ibid.* **128**, 2267 (1962).

⁴M. Gell-Mann and K. A. Brueckner, *Phys. Rev.* **106**, 364 (1957).

⁵H. P. Kelly, *Phys. Rev.* **131**, 684 (1963).

⁶H. P. Kelly, *Phys. Rev.* **136**, B896 (1964).

single-particle wave functions φ_n , which are solutions of

$$(T+V)\varphi_n = \epsilon_n \varphi_n, \quad (6)$$

constitute an orthonormal set. The wave function Φ_0 is a determinant of the N solutions of Eq. (6) which are lowest in energy. The states occupied in Φ_0 are called unexcited states. The remaining single-particle states of the orthonormal set are called excited states. The unoccupied unexcited states are called holes and the occupied excited states are called particles. The correct ground-state wave function Ψ_0 and energy E are obtained by perturbing the approximate Φ_0 by

$$H' = H - H_0 = \sum_{i < j}^N v_{ij} - \sum_{i=1}^N V_i, \quad (7)$$

and we obtain²

$$\Psi_0 = \lim_{\alpha \rightarrow 0} U_\alpha(0)\Phi_0 / \langle \Phi_0 | U_\alpha(0) | \Phi_0 \rangle, \quad (8)$$

and

$$E = E_0 + \langle \Phi_0 | H' | \Psi_0 \rangle, \quad (9)$$

where

$$U_\alpha(t) = \sum_{n=0}^{\infty} (-i)^n \times \int_{t > t_1 > t_2 \dots > t_n} H'(t_1) \dots H'(t_n) dt_1 \dots dt_n, \quad (10)$$

and

$$H'(t) = e^{iH_0 t} H' e^{-iH_0 t} e^{\alpha t}. \quad (11)$$

In the matrix element representation,

$$H_0 = \sum_n \epsilon_n \eta_n^\dagger \eta_n, \quad (12)$$

and

$$H' = \frac{1}{2} \sum_{pqmn} \langle pq | v | mn \rangle \eta_p^\dagger \eta_q^\dagger \eta_n \eta_m - \sum_{pm} \langle p | V | m \rangle \eta_p^\dagger \eta_m. \quad (13)$$

The operators η^\dagger and η satisfy the usual Fermi-Dirac anticommutation relations.² Wick's theorem may be used to express $U_\alpha(0)$ by sums of terms, each of which may be expressed by a Feynman-type diagram.²

The term $U_\alpha(0)$ may be expressed as a product of a sum of "linked" terms and a sum of "unlinked" terms equal to $\langle \Phi_0 | U_\alpha(0) | \Phi_0 \rangle$. After the time integrations in Eq. (10) have been carried out, one obtains the result

$$\Psi_0 = \sum_L \left(\frac{1}{E_0 - H_0} H' \right)^n \Phi_0, \quad (14)$$

where \sum_L means that only "linked" terms are to be included.² Also,

$$E - E_0 = \Delta E = \sum_{L'} \langle \Phi_0 | H' \left(\frac{1}{E_0 - H_0} H' \right)^n | \Phi_0 \rangle, \quad (15)$$

where L' restricts the sum to those terms which are "linked" when the leftmost H' interaction is removed for $n \geq 1$.

III. SYMMETRIES

In deriving Eq. (14) for Ψ_0 , the factor $\langle \Phi_0 | U_\alpha(0) | \Phi_0 \rangle$ contained in $U_\alpha(0)\Phi_0$ cancels the same factor in the denominator of Eq. (8). The time integrations are then carried out and give

$$\Psi_0 = \lim_{\alpha \rightarrow 0} \left(1 + \frac{1}{E_0 - H_0 + i\alpha} H' + \frac{1}{E_0 - H_0 + i2\alpha} H' \frac{1}{E_0 - H_0 + i\alpha} H' + \dots \right)_L \Phi_0. \quad (16)$$

Since only "linked" terms are included in Eq. (16), excited states must be included as the intermediate states after H' operates on Φ_0 . When all excited single-particle states have energies greater than those of the unexcited states, then $E_0 - H_0$ in Eq. (16) cannot vanish and we may take the limit $\alpha \rightarrow 0$ which gives the result of Eq. (14). This is the reason for Goldstone's statement that he assumes that H_0 has a nondegenerate ground state Φ_0 and that his proof applies only to the ground state of a closed-shell nucleus.

A general extension of the linked diagram expansion for the degenerate ground state of a system of fermions has been made by Bloch and Horowitz.⁸ However, in many cases it is possible to make use of the Brueckner-Goldstone (BG) expansion directly even though we are dealing with open-shell systems with degenerate ground states. This is because the conserved quantum numbers may prevent the perturbation from leading to excited states [here we mean N -particle states which occur after H' in Eq. (16)] which are degenerate with the ground state.

For example, let us assume L - S coupling and start from an unperturbed ground state Φ_0 specified by quantum numbers L, M_L, S, M_S . The operators L_\pm, L_z, S_\pm, S_z commute with the term $\sum v_{ij}$ of the perturbation for v_{ij} equal to $v(|\mathbf{r}_i - \mathbf{r}_j|)$ and spin-independent, as is the case for Coulomb interactions. These operators also commute with $\sum V_i$ when V is independent of the single-particle quantum numbers m_l and m_s . That is, V must be spherically symmetric and spin-independent. Then L_\pm, L_z, S_\pm, S_z commute with the perturbation H' . If we start with Φ_0 , an eigenstate of L^2, L_z, S^2, S_z , then the perturbation can only lead to those excited single-particle states which give a total N -particle excited state with the same eigenvalues of L^2, L_z, S^2, S_z as Φ_0 . The usual degeneracies in M_L and M_S in open-shell atoms are now avoided. When the ground state is uniquely specified by the electronic configuration and the quantum numbers L, M_L, S , and M_S as for most atoms, then we may be able to apply the BG expansion directly.

In the usual description of the BG perturbation expansion it is assumed that the unperturbed ground-state

⁸ C. Bloch and J. Horowitz, Nucl. Phys. 8, 91 (1958).

wave function Φ_0 is a single determinant, but in general for open-shell atoms Φ_0 is not necessarily a single determinant. However, in many open-shell cases if one chooses $M_L = \pm L$ and $M_S = \pm S$ then Φ_0 is a single determinant. The reason for this is due to Hund's rule according to which the atomic ground state has the largest spin of those terms which may be formed from the ground-state configuration.⁹ Since the total energy, for example, is independent of the choice of M_L and M_S , in calculating such quantities as the correlation energy it is often possible to choose Φ_0 as a single determinant as will be shown for oxygen. When the state Φ_0 is a linear combination of determinants, we also may be able to carry out the BG expansion. Again we allow $U_\alpha(0)$ to act on Φ_0 and then we factor out $\langle \Phi_0 | U_\alpha(0) | \Phi_0 \rangle$ which cancels the denominator of Eq. (8). The result is that those combinations of single-particle states which enter into Φ_0 are again excluded as intermediate N -particle states in the perturbation expansion.

As an explicit example, let us consider the ground state of neutral carbon which is $(1s)^2(2s)^2(2p)^2\ ^3P$. The ground state is given by the single determinant (1^+0^+) . The notation 1^+ refers to a single $2p$ electron with $m_l = +1$ and $m_s = +\frac{1}{2}$ and 0^+ refers to a $2p$ electron with $m_l = 0$ and $m_s = +\frac{1}{2}$. It is understood that this determinant also contains two $1s$ electrons with $m_s = \pm\frac{1}{2}$ and likewise two $2s$ states with $m_s = \pm\frac{1}{2}$. This notation is that used by Slater.¹⁰ The BG expansion may now be applied to $\Phi_0 = (+1^+0^+)$. The excited $2p$ states (-1^+) , $(+1^-)$, (0^-) , and (-1^-) which are degenerate in energy with $(+1^+)$ and (0^+) are not reached by the perturbation because of conservation of M_L and M_S . That is, they cannot be the only excitations present. It is possible, for example, to excite $2p(+1^+)$ and $2p(0^+)$ into $4f(+2^+)$ and $2p(-1^+)$, respectively. However, there is no problem of vanishing energy denominators in this case. If we choose the carbon ground state

$$\Phi_0(^3P; M_L=0, M_S=0) = (1/\sqrt{2})[(+1^-1^+) + (+1^+-1^-)], \quad (17)$$

the operator $U_\alpha(0)$ applied to Eq. (17) gives $2p$ intermediate states with vanishing denominators but they add to give Φ_0 which may be projected out as has been discussed. For example, in first order, the Coulomb perturbation $\frac{1}{2} \sum \langle pq | v | mn \rangle \eta_p^\dagger \eta_q^\dagger \eta_n \eta_m$ applied to Φ_0 gives terms with vanishing denominators when $p, q, m,$ and n refer to the $2p$ states. The first-order correction to Φ_0 with denominator $i\alpha$ from the Coulomb part of $U_\alpha(0)\Phi_0$ is

$$U_\alpha(0)_{c1}(+1^-1^+) = (i\alpha)^{-1}[(F_0 + (1/25)F_2) \times (+1^-1^+) - (3/25)F_2(0^-0^+) + (6/25)F_2(-1^-+1^+)], \quad (18)$$

⁹ E. U. Condon and G. H. Shortley, *The Theory of Atomic Spectra* (Cambridge University Press, Cambridge, 1957), p. 209.

¹⁰ J. C. Slater, *Quantum Theory of Atomic Structure* (McGraw-Hill Book Company, Inc., New York, 1960), Vol. II, Chap. 20, p. 84.

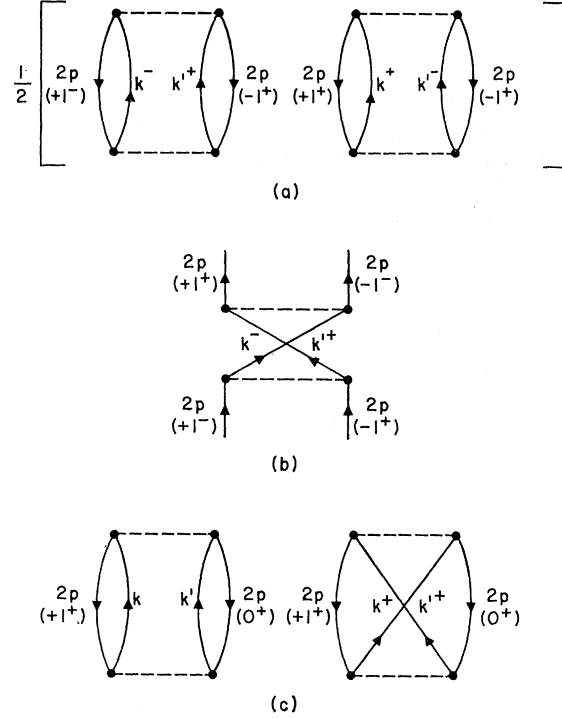


FIG. 1. Second-order correlation energy diagrams for the 3P ground state of carbon. Direct diagrams (a) and exchange diagram (b) for $\Phi_0(^3P; M_L=0, M_S=0)$. (c) Diagrams for $\Phi_0(^3P; M_L=L, M_S=S)$.

$$U_\alpha(0)_{c1}(+1^+-1^-) = (i\alpha)^{-1}[(F_0 + (1/25)F_2) \times (+1^+-1^-) - (3/25)F_2(0^+0^-) + (6/25)F_2(-1^++1^-)],$$

where

$$F_k = \int_0^\infty \int_0^\infty \frac{r < k}{r > k+1} P_{2p}^2(r_1) P_{2p}^2(r_2) dr_1 dr_2. \quad (19)$$

The angular integrations were obtained from Ref. 9, p. 178. Since $(0^-0^+) = -(0^+0^-)$ and $(-1^-+1^+) = -(+1^+-1^-)$, we obtain

$$U_\alpha(0)_{c1}\Phi_0 = (i\alpha)^{-1}(F_0 - 5/25F_2)\Phi_0. \quad (20)$$

The first-order part of $U_\alpha(0)\Phi_0$ with denominator $i\alpha$ due to the term $-\sum \langle m | V | p \rangle \eta_m^\dagger \eta_p$ also is proportional to Φ_0 . All these terms vanish when we project out $\langle \Phi_0 | U_\alpha(0) | \Phi_0 \rangle$.

When the correlation energy is calculated for the carbon ground state $\Phi_0(^3P; M_L=0, M_S=0)$ of Eq. (17) there will be cross terms between the two determinants. Second-order energy terms for $2p$ electron correlations are shown in Figs. 1(a) and 1(b). The diagram of Fig. 1(b) describes the cross term between the two determinants. The diagrams are given according to Goldstone's notation.² There is a minus sign associated with the diagram of Fig. 1(b). The states k and k' are all the allowed excited states. Those $2p$ excitations with vanishing denominators are excluded as dis-

cussed. Second-order correlation energy diagrams for $\Phi_0(^3P; M_L=L, M_S=S)$ are shown in Fig. 1(c). The contributions of the diagrams shown in Figs. 1(a) and 1(b) must equal the contributions shown in Fig. 1(c), and this has been explicitly verified by enumeration of the angular coefficients.¹¹ However, the exchange contribution of Fig. 1(b) is not equal to the exchange diagram shown in Fig. 1(c).

The atom chosen for the numerical calculations is neutral oxygen $(1s)^2(2s)^2(2p)^4\ ^3P$ which is similar to carbon. The 3P ground state may be represented by a single determinant¹⁰:

$$\Phi_0(^3P; M_L=L, M_S=S) = (+1+0^+ - 1^+ + 1^-). \quad (21)$$

The BG expansion may again be applied directly and it is found that there are no vanishing energy denominators due to conservation of M_L and M_S by the perturbation. The perturbation could also have been applied to the other 3P states such as

$$\begin{aligned} \Phi_0(^3P; M_L=0, M_S=0) \\ = (1/\sqrt{2})[(+1-0^+ - 1^+ 0^-) + (+1+0^+ - 1^- 0^-)]. \quad (22) \end{aligned}$$

IV. CHOICE OF POTENTIAL

In order to obtain the Φ_0 which is the best approximation to the exact ground-state wave function Ψ_0 , a minimization of $\langle \Phi_0 | H | \Phi_0 \rangle$ subject to the usual orthonormality constraints is carried out.¹⁰ The single-particle states of Φ_0 then satisfy the well-known Hartree-Fock (HF) equations

$$\begin{aligned} -\frac{1}{2}\nabla^2\varphi_n(\mathbf{r}) - \frac{Z}{r}\varphi_n(\mathbf{r}) \\ + \left(\sum_{j=1}^N \int \frac{d\mathbf{r}'\varphi_j^*(\mathbf{r}')\varphi_j(\mathbf{r}')}{|\mathbf{r}-\mathbf{r}'|} \right) \varphi_n(\mathbf{r}) \\ - \sum_{j=1}^N \left(\delta(m_{s_n}, m_{s_j}) \int \frac{d\mathbf{r}'\varphi_j^*(\mathbf{r}')\varphi_n(\mathbf{r}')}{|\mathbf{r}-\mathbf{r}'|} \varphi_j(\mathbf{r}) \right) \\ = \epsilon_n \varphi_n(\mathbf{r}). \quad (23) \end{aligned}$$

The terms involving φ_j represent the Hartree-Fock potential V_{HF} acting on φ_n . This potential may be represented in terms of its matrix elements

$$\langle a | V_{\text{HF}} | b \rangle = \sum_{n=1}^N (\langle an | v | bn \rangle - \langle an | v | nb \rangle). \quad (24)$$

The coupled equations (23) must be solved self-consistently to obtain the N single-particle states φ_n of Φ_0 . At this point, V_{HF} , which is nonlocal and Hermitian, is determined.

For open-shell atoms, in general one does not have spherical symmetry and therefore the solutions of Eq.

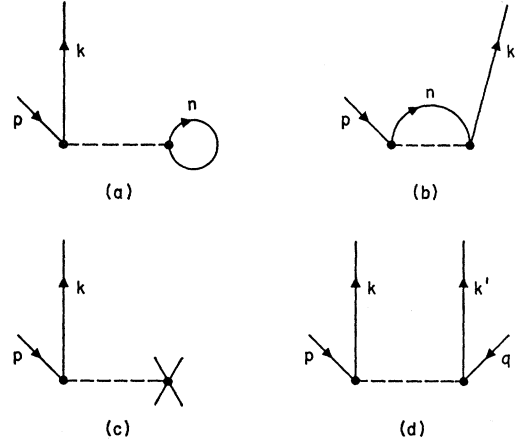


Fig. 2. First-order corrections to the unperturbed wave function Φ_0 . (a) Direct interaction with passive unexcited state n . This term equals $(\epsilon_p - \epsilon_k)^{-1} \langle km | v | pn \rangle \times \eta_k^+ \eta_p | \Phi_0 \rangle$. (b) Exchange interaction with n . (c) Interaction with the potential V . (d) Two-body correlation correction. The states n are summed over all unexcited states. When the Hartree-Fock potential of Eq. (24) is used to calculate the unexcited states, the diagrams (a), (b), and (c) add to zero.

(23) cannot always be written

$$\varphi_n(\mathbf{r}) = R_{nl}(r) Y_{lm}(\theta, \varphi) \chi_s(m_s). \quad (25)$$

It is extremely difficult then to obtain exact solutions of Eq. (23). This difficulty is avoided by assuming that each single-particle state has the form of Eq. (25). The quantity $\langle \Phi_0 | H | \Phi_0 \rangle$ is then minimized with respect to all R_{nl} subject to the usual orthonormality constraints. The resulting "restricted" HF equations may be solved in practice and the "restricted" V_{HF} is now spherically symmetric. This procedure has the advantage that it is practical and in addition, since the single-particle radial functions R_{nl} are independent of m_l and m_s , Φ_0 may be constructed as an eigenstate of L^2 , L_Z , S^2 , and S_Z which would not necessarily be possible if the solutions of Eq. (23) were used for open-shell atoms.

In applying the BG theory it is necessary to obtain a complete basis set of single-particle states. A Hartree-Fock basis set may be obtained by calculating all solutions of Eq. (23). Those N states lowest in energy are the unexcited states of Φ_0 . For the bound excited states it is only necessary to calculate a finite number as suitable extrapolations may be made to account for the remaining bound states of high principal quantum number.⁶ For continuum states, it is only necessary to calculate a sufficient number to carry out all numerical integrations with the desired accuracy.

An advantage in using the HF basis set is that Φ_0 is optimized. In the BG theory there are first-order corrections to Φ_0 as shown in Figs. 2(a), 2(b), 2(c), and 2(d). With the HF basis, the correction term due to V_{HF} in Fig. 2(c) cancels the terms shown in Figs. 2(a) and 2(b). To first order, then, there are no corrections

¹¹ Reference 9, p. 178.

to Φ_0 involving only single excitations when the HF basis is used. This only holds true when Eq. (23) is used for the HF states. For atoms lacking spherical symmetry, the "restricted" HF procedure does not result in the exact cancellation of the terms shown in Figs. 2(a), 2(b), and 2(c). However, the cancellation with the "restricted" HF basis may be very good so that the principal first-order correction to Φ_0 is the true correlation correction of Fig. 2(d). The diagrams of Figs. 2(a), 2(b), and 2(c) may also be easily calculated. The cancellation was found to be quite good in the oxygen calculations described in the next section.

When the HF basis of Eq. (23) is used, the excited single-particle states do not correspond to physical single-particle excitations of the atom.⁵ When we calculate unexcited states φ_n by Eq. (23), the direct and exchange terms cancel for j equal to n . The state φ_n is then calculated in the field of the nucleus and $N-1$ other electrons. For excited states there is no cancellation and the HF excited states are calculated in the field of the nucleus and N other electrons. For neutral atoms this leads to the possibility that all the excited states may lie in the continuum. There were no bound excited states in the previous beryllium calculation

with the HF basis, and it was argued that this will be the case for most if not all neutral atoms.⁵ A search for these bound, excited HF states in neutral oxygen also gave negative results. The advantage of eliminating bound excited states is offset, however, by the resulting slow convergence of the perturbation expansion as found in Ref. 5. It was pointed out in Ref. 6 that excited states have interactions with $N-1$ other electrons and it is therefore desirable to calculate these excited states in the potential field of $N-1$ other electrons. This type of potential was used in Ref. 6 and the convergence of the BG expansion for the beryllium correlation energy was greatly improved. The same arguments also apply in the case of "restricted" HF potentials for open-shell atoms.

In Ref. 6 the potential V was chosen by calculating all states in the fixed field of neutral beryllium minus one of the $2s$ electrons. Hartree-Fock states were used to calculate this fixed potential. In this potential the $2s$ state is the HF $2s$ state, but the $1s$ state differs very slightly from the HF $1s$ wave function. The same prescription is used in this paper to obtain the set of single-particle states for oxygen. The equation for the radial functions $P_{nl}(r) = rR_{nl}(r)$ for $l=0$ is

$$\left(-\frac{1}{2} \frac{d^2}{dr^2} - \frac{8}{r}\right) P_{n0}(r) + 2 \int_0^\infty dr' P_{1s}^2(r') v_0(r, r') P_{n0}(r) - \int_0^\infty dr' P_{1s}(r') P_{n0}(r') v_0(r, r') P_{1s}(r) + \int_0^\infty dr' P_{2s}^2(r') v_0(r, r') P_{n0}(r) + 4 \int_0^\infty dr' P_{2p}^2(r') v_0(r, r') P_{n0}(r) - \frac{2}{3} \int_0^\infty dr' P_{2p}(r') P_{n0}(r') v_1(r, r') P_{2p}(r) = \epsilon_{n0} P_{n0}(r), \quad (26)$$

where

$$v_K(r, r') = r_{<^K} / r_{>^{K+1}}, \quad (27)$$

$r_{<}$ being the lesser of r and r' , and $r_{>}$ being the greater of r and r' . For $l=1$ states the radial equation is

$$\left[\frac{1}{2} \left(-\frac{d^2}{dr^2} + \frac{2}{r^2}\right) - \frac{8}{r}\right] P_{n1}(r) + 2 \int_0^\infty dr' P_{1s}^2(r') v_0(r, r') P_{n1}(r) - \frac{1}{3} \int_0^\infty dr' P_{1s}(r') P_{n1}(r') v_1(r, r') P_{1s}(r) + 2 \int_0^\infty dr' P_{2s}^2(r') v_0(r, r') P_{n1}(r) - \frac{1}{3} \int_0^\infty dr' P_{2s}(r') P_{n1}(r') v_1(r, r') P_{2s}(r) + 3 \int_0^\infty dr' P_{2p}^2(r') v_0(r, r') P_{n1}(r) - \frac{3}{50} \int_0^\infty dr' P_{2p}^2(r') v_2(r, r') P_{n1}(r) - \frac{6}{25} \int_0^\infty dr' P_{2p}(r') P_{n1}(r') v_2(r, r') P_{2p}(r) = \epsilon_{n1} P_{n1}(r). \quad (28)$$

When oxygen HF orbitals are used for P_{1s} , P_{2s} , and P_{2p} , Eqs. (26) and (28) are the oxygen HF equations for $P_{2s}(r)$ and $P_{2p}(r)$, respectively.¹² The lowest energy solution of Eq. (26) is a $1s$ orbital but it is not the HF $1s$ solution. It is, however, a good approximation to the HF P_{1s} . The next lowest energy solution to Eq. (26) is the HF P_{2s} . In

¹² D. R. Hartree, W. Hartree, and B. Swirles, Phil. Trans. Roy. Soc. (London) A238, 229 (1940).

Eq. (26) we are calculating $l=0$ states in the field of neutral oxygen minus one $2s$ electron; in Eq. (28) we are calculating $l=1$ states in the field of neutral oxygen minus one $2p$ electron. The solutions of Eqs. (26) and (28) give orthogonal sets of $l=0$ and $l=1$ single-particle wave functions.

The choice of equations for $l>1$ is slightly more arbitrary than for $l=0$ and 1. It is desirable to calculate the $l>1$ states in the HF field of oxygen with one $2p$ electron removed. The $2p$ exchange coefficient was estimated as that which would cause as much cancellation as possible of the interactions with the passive unexcited states in the perturbation expansion.² For $l=2$, the equation for this investigation is

$$\begin{aligned} & \left[\frac{1}{2} \left(-\frac{d^2}{dr^2} + \frac{6}{r^2} \right) - \frac{8}{r} \right] P_{n2}(r) + 2 \int_0^\infty dr' P_{1s}^2(r') v_0(r, r') P_{n2}(r) - \frac{1}{5} \int_0^\infty dr' P_{1s}(r') P_{n2}(r') v_2(r, r') P_{1s}(r) \\ & + 2 \int_0^\infty dr' P_{2s}^2(r') v_0(r, r') P_{n2}(r) - \frac{1}{5} \int_0^\infty dr' P_{2s}(r') P_{n2}(r') v_2(r, r') P_{2s}(r) \\ & + 3 \int_0^\infty dr' P_{2p}^2(r') v_0(r, r') P_{n2}(r) - 0.11 \int_0^\infty dr' P_{2p}(r') P_{n2}(r') v_3(r, r') P_{2p}(r) = \epsilon_{n2} P_{n2}(r). \quad (29) \end{aligned}$$

For $l=3$, P_{n3} in this calculation is determined by

$$\begin{aligned} & \left[\frac{1}{2} \left(-\frac{d^2}{dr^2} + \frac{12}{r^2} \right) - \frac{8}{r} \right] P_{n3}(r) + 2 \int_0^\infty dr' P_{1s}^2(r') v_0(r, r') P_{n3}(r) - \frac{1}{7} \int_0^\infty dr' P_{1s}(r') P_{n3}(r') v_3(r, r') P_{1s}(r) \\ & + 2 \int_0^\infty dr' P_{2s}^2(r') v_0(r, r') P_{n3}(r) - \frac{1}{7} \int_0^\infty dr' P_{2s}(r') P_{n3}(r') v_3(r, r') P_{2s}(r) \\ & + 3 \int_0^\infty dr' P_{2p}^2(r') v_0(r, r') P_{n3}(r) - 0.10 \int_0^\infty dr' P_{2p}(r') P_{n3}(r') v_2(r, r') P_{2p}(r) = \epsilon_{n3} P_{n3}(r). \quad (30) \end{aligned}$$

Equations (26), (28), (29), and (30) were solved numerically to obtain the $l=0, 1, 2$, and 3 single-particle wave functions used in the perturbation expansion. Hartree-Fock orbitals were used for P_{1s} , P_{2s} , and P_{2p} in Eqs. (26), (28), (29), and (30). These HF orbitals were obtained by iterating several times the oxygen HF solutions of Hartree, Hartree, and Swirles¹² in order to obtain greater accuracy. The resulting orbitals were found to be in excellent agreement with the accurate analytic HF solutions of Bagus and Roothaan and differed from the Bagus-Roothaan solutions by one or two digits in the fourth decimal place.¹³ The $1s$ solution of Eq. (26) was found to be quite close to the HF $1s$ solution although calculated by a different potential. The $1s$ solution of Eq. (26) is compared in Table I with the HF $1s$ solution obtained by iterating the solution of Ref. 12 and with the HF $1s$ solution of Bagus and Roothaan.¹³ Both the $1s$ orbital of Eq. (26) and the HF $1s$ orbital are strictly orthogonal to the HF $2s$ orbital.

The difference between $\langle \Phi_0 | H | \Phi_0 \rangle$ calculated with P_{1s} of Eq. (26) and with the P_{1s} HF is extremely small since $\langle \Phi_0 | H | \Phi_0 \rangle$ is stationary with respect to variations in Φ_0 . This difference, which was calculated most accurately by perturbation theory, was found to be

0.0000215 a.u. One a.u. equals 27.21 eV. By comparison, $\langle \Phi_0 | H | \Phi_0 \rangle = -74.80936$ a.u. is the HF result of Bagus and Roothaan. It is interesting, however, to note that ϵ_{1s} (-21.726 a.u.) does differ significantly from ϵ_{1s} .

TABLE I. Radial functions $P_{1s}(r)$ for oxygen.

r	$P_{1s}(r)^a$	$P_{1s}(r)^b$	$P_{1s}(r)^c$
0.01	0.39819	0.39841	0.39848
0.04	1.25498	1.25566	1.25560
0.08	1.83251	1.83339	1.83336
0.10	1.95985	1.96069	1.96072
0.12	2.01383	2.01457	2.01465
0.14	2.01336	2.01394	2.01404
0.16	1.97319	1.97359	1.97367
0.20	1.81724	1.81726	1.81726
0.24	1.61023	1.60990	1.60982
0.28	1.38982	1.38922	1.38912
0.30	1.28164	1.28094	1.28085
0.34	1.07726	1.07645	1.07640
0.40	0.81167	0.81086	0.81090
0.50	0.48605	0.48552	0.48561
0.80	0.09021	0.09041	0.09033
1.00	0.02853	0.02875	0.02870
1.40	0.00348	0.00356	0.00362
2.00	0.00037	0.00046	0.00051
2.60	0.00006	0.00010	0.00012
3.00	0.00003	0.00004	0.00004
$-\epsilon_{1s}$ (a.u.)	21.72625	20.66908	20.66860

^a The $1s$ orbital calculated from Eq. (26). This orbital was not calculated in the HF potential and differs slightly from the Hartree-Fock P_{1s} .

^b Hartree-Fock $P_{1s}(r)$ calculated by iterating the HF oxygen solutions of Ref. 12.

^c Hartree-Fock $P_{1s}(r)$ obtained from analytic solutions of Bagus and Roothaan.

¹³ I am very grateful to Dr. P. S. Bagus and Professor C. C. J. Roothaan for kindly sending me a detailed listing of their Hartree-Fock results for oxygen.

HF (-20.669 a.u.). This is understood by considering that in Eq. (26) the potential for P_{1s} has two direct interactions and one exchange interaction with P_{1s} HF and one direct interaction with P_{2s} in addition to the interactions with P_{2p} . When we solve for P_{1s} , the $1s$ exchange interaction very nearly cancels one direct $1s$ interaction and the net effect is that P_{1s} has one direct $1s$ interaction and one direct $2s$ interaction in addition to the $2p$ interactions. In the HF case, P_{1s} HF (hereafter denoted P_{1s}') has one direct $1s$ interaction, two direct $2s$ interactions, and one exchange $2s$ interaction in addition to $2p$ interactions. Since P_{1s} lacks one direct and one exchange interaction with P_{2s} as compared with P_{1s}' , it is expected to be lower in energy since the positive direct term is generally larger than the negative exchange term. The difference between ϵ_{1s} and the HF ϵ_{1s}' is readily corrected when we use P_{1s} in the perturbation expansion. Whenever the $1s$ state appears in the perturbation expansion there are corresponding higher order terms which account for $1s$ interactions with the other occupied unexcited states and with the potential V . A typical first-order correction to Φ_0 involving a $1s$ hole line is shown in Fig. 3(a). In the next order the $1s$ hole line is modified by direct and exchange interactions with the passive unexcited states as shown in Figs. 3(b) and 3(c). The $1s$ hole line is also modified by interaction with the potential V as shown in Fig. 3(d). The corrections to the term of Fig. 3(a) shown in Figs. 3(b), 3(c), and 3(d) are given by $-v/D$ times the term of Fig. 3(a), where v is the sum of the matrix elements of the interactions shown in Figs. 3(b), 3(c), and 3(d) and D is the same denominator as in Fig. 3(a). The nondiagonal terms, which are much smaller, are calculated separately. The minus sign comes from the additional hole line. In third and higher orders these interactions are again repeated, the m th correction being the term of Fig. 3(a) multiplied by $(-v/D)^m$. These terms add geometrically and the result is that the term of Fig. 3(a) is multiplied by $(1+v/D)^{-1}$ which is equivalent to replacing D by $D+v$ in Fig. 3(a). When V_{HF} is used, v is zero. However, these terms are not zero when the restricted HF solution is used for open-shell atoms. For example, in oxygen for $\Phi_0 = (+1^+0^+ - 1^+ + 1^-)$, v is different for $1s^+$ and $1s^-$ because $1s^+$ has exchange interactions with three $2p$ electrons and $1s^-$ has only one $2p$ exchange term, whereas the restricted HF potential for both $1s$ states has exchange interactions with two $2p$ electrons. If we consider these $1s-2p$ corrections due to use of a restricted HF potential separately, then the correction v for $1s$ states due to the use of Eq. (26) is

$$v = \langle 1s1s | v | 1s1s \rangle + 2\langle 2s1s | v | 2s1s \rangle - \langle 2s1s | v | 1s2s \rangle - [2\langle 1s1s' | v | 1s1s' \rangle - \langle 1s1s' | v | 1s'1s \rangle + \langle 2s1s | v | 2s1s \rangle]. \quad (31)$$

The term in square brackets comes from the choice of potential used in Eq. (26) and $1s'$ is the HF $1s$ orbital

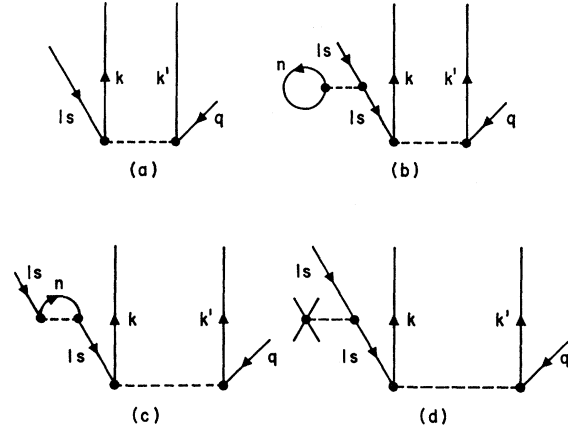


FIG. 3. (a) First-order correction to Φ_0 involving $1s$ state. (b) Direct interaction of $1s$ hole line with the passive unexcited state n . (c) Exchange interaction of $1s$ hole line with n . (d) Interaction of $1s$ hole state with the potential V .

used in Eq. (26). Since the same type of correction may be made for each hole line, we simply add the appropriate v to each single-particle energy ϵ . Using the matrix elements listed in Table II, we find that v for ϵ_{1s} is 1.05572 and $\epsilon_{1s} + v$ is -20.6705 a.u. as compared with the HF $\epsilon_{1s}' = -20.66908$ a.u.

V. CORRELATION ENERGIES

A. Second-Order Calculations

The BG perturbation expansion may be used to obtain both the ground-state energy E and wave function ψ_0 . The energy E may often be obtained from experiment and this serves as a check on the accuracy of the calculations. The correlation energy is defined by

$$E_{\text{corr}} = E - E_{\text{HF}}. \quad (32)$$

TABLE II. Matrix elements among unexcited states.^a

$\langle 1s1s v 1s1s \rangle$	4.73865
$\langle 1s'1s' v 1s'1s' \rangle^b$	4.74118
$\langle 1s1s' v 1s1s' \rangle$	4.73992
$\langle 1s1s' v 1s'1s \rangle$	4.73991
$\langle 2s1s v 2s1s \rangle$	1.13425
$\langle 2s1s v 1s2s \rangle$	0.07726
$\langle 2s1s' v 2s1s' \rangle$	1.13430
$\langle 2s1s' v 1s'2s \rangle$	0.07733
$\langle 2s2s v 2s2s \rangle$	0.79794
$\langle 2s2p v 2s2p \rangle$	0.77387
$\langle 2s2p v 2p2s \rangle$	0.47214
$\langle 2p1s v 2p1s \rangle$	1.09845
$\langle 2p1s v 1s2p \rangle$	0.105655
$\langle 2p1s' v 2p1s' \rangle$	1.098464
$\langle 2p1s' v 1s'2p \rangle$	0.105583
$\langle 2p2p v 2p2p \rangle$	$\begin{cases} 0.754853 (k=0)^c \\ 0.336095 (k=2) \end{cases}$

^a Only the radial parts of the matrix elements are given.

^b The states $1s'$, $2s$, and $2p$ are Hartree-Fock states. The $1s$ state was calculated from Eq. (26).

^c The notation k is defined in Eq. (27).

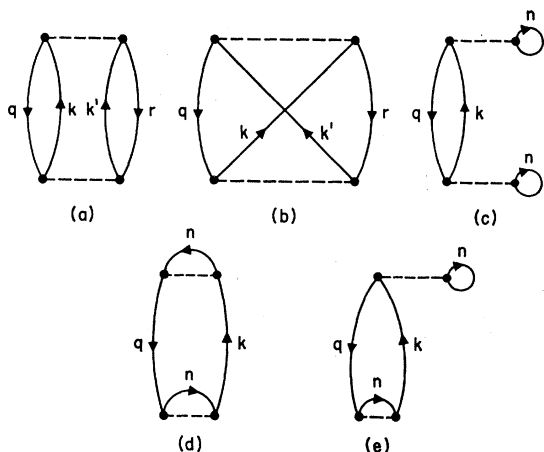


FIG. 4. Second-order energy diagrams. (a) Direct correlation diagram. (b) Exchange. (c), (d), and (e) are single-excitation diagrams. We may also have the order of exchange and direct interactions interchanged in (e). There are also diagrams like (c), (d), and (e) with interactions with the potential V . These single-excitation diagrams add to zero when a completely unrestricted Hartree-Fock potential is used.

The energy E may be obtained by adding the experimental ionization potentials and subtracting the estimated relativistic contributions to the total energy. A more accurate procedure is to use the experimental ionization potentials for all but the last two electrons and then use Pekeris' calculations¹⁴ to obtain the remaining energy. The relativistic energy among the first $N-2$ electrons is then subtracted to obtain E . Clementi has given the correlation energies for a large number of atoms and for the 3P ground state of neutral oxygen he has obtained $E_{\text{corr}} = -0.258$ a.u. with an estimated accuracy of 5%.¹⁵ The relativistic contribution is approximately -0.0503 a.u. and $E_{\text{HF}} = -74.80936$ a.u.¹⁵ The HF solution in this case is the restricted HF solution described in Sec. IV and described in detail by Roothaan.¹⁶ As will be seen from the perturbation calculations, the energy difference between the restricted HF solution and a completely unrestricted HF solution is very small compared to the energy corrections from true two-body correlations.

Given the unperturbed state Φ_0 , we may calculate

$$\langle \Phi_0 | H | \Phi_0 \rangle = E_0 + E_1,$$

where E_0 is given by Eq. (5) and $E_1 = \langle \Phi_0 | H' | \Phi_0 \rangle$. When Φ_0 is the HF solution, $E_0 + E_1$ is the HF energy E_{HF} . The lowest order energy corrections to $\langle \Phi_0 | H | \Phi_0 \rangle$ are second-order terms which are shown in Fig. 4. When a fully unrestricted HF basis is used, the diagrams of Figs. 4(c), 4(d), and 4(e) and the corresponding inter-

actions with V_{HF} add to zero. As discussed in Sec. IV, for open-shell atoms we must use a "restricted" HF basis and so there are contributions to the energy from diagrams as shown in Figs. 4(c), 4(d), and 4(e). However, it is found that they are quite small compared to the diagrams of Figs. 4(a) and 4(b).

The diagrams of Fig. 4 are calculated according to the rules given in Ref. 2. For example, the diagram of Fig. 4(a), which describes correlations among electrons in states q and r , is given by

$$E_2^{(a)}(q,r) = \sum_{k,k'} \frac{\langle qr | v | kk' \rangle \langle kk' | v | qr \rangle}{\epsilon_q + \epsilon_r - \epsilon_k - \epsilon_{k'}}. \quad (33)$$

The sums are over all excited states. Bound excited states are labeled by the principal quantum number n , orbital angular momentum l , azimuthal quantum number m_l , and spin projection m_s . In practice, the sums over n are carried out explicitly for the first eight or ten excited states and the remaining infinite sum may be carried out by integration as shown in Ref. 6, since

$$\lim_{n \rightarrow \infty} \langle m_l n l' | v | q r \rangle = n^{-3/2} \times \text{const}, \quad (34)$$

$$n \rightarrow \infty, m \text{ fixed.}$$

The sums over m_l and m_s are carried out for each l value. The previous beryllium calculation⁵ included $l=0, 1$, and 2 states and the present oxygen calculation includes $l=0, 1, 2$, and 3 states. The continuum states are labeled by k, l, m_l , and m_s , where $\epsilon_k = k^2/2$. If the atom is enclosed in a large spherical volume of radius R_0 where R_0 tends to infinity, then

$$P_{kl}(r) = (2/R_0)^{1/2} \cos[kr + \delta_l - 1/2(l+1)\pi], \quad (35)$$

for large r . Since P_{kl} must vanish for $r=R_0$,

$$kR_0 + \delta_l - \frac{1}{2}(l+1)\pi = n\pi, \quad (36)$$

where n is an integer. For fixed l , the number of states Δn in the range Δk is determined by

$$\Delta k R_0 + \Delta \delta_l = \Delta n \pi. \quad (37)$$

Since $\Delta \delta_l / R_0 \rightarrow 0$ for $R_0 \rightarrow \infty$, we obtain

$$\Delta n = (R_0/\pi) \Delta k, \quad (38)$$

and

$$\sum_k = (R_0/\pi) \int_0^\infty dk. \quad (39)$$

The normalization factor $(2/R_0)^{1/2}$ may then be omitted from Eq. (35) and the summation of Eq. (39) changed to

$$\sum_k = \left(\frac{2}{\pi}\right) \int_0^\infty dk. \quad (40)$$

Sums over l, m_l , and m_s must still be carried out.

¹⁴ C. L. Pekeris, Phys. Rev. **112**, 1649 (1958).

¹⁵ E. Clementi, J. Chem. Phys. **38**, 2248 (1963). This value of E_{corr} for oxygen may be obtained by adding the nonrelativistic ionization potentials as given by C. W. Scherr, J. N. Silverman, and F. A. Matsen, Phys. Rev. **127**, 830 (1962). Then E_{HF} is subtracted to give E_{corr} .

¹⁶ C. C. J. Roothaan, Rev. Mod. Phys. **32**, 179 (1960).

B. Higher Order Diagrams

In Ref. 5 it was found necessary to include terms beyond second order when the HF basis set is used. However, it was shown in Ref. 6 that the second-order results are closer to the correct value when the basis set is used in which excited states are calculated in the field of the nucleus and $N-1$ other electrons, which is the basis set used in this paper. Nevertheless, it is still desirable to include the effects of terms beyond second order. Neglecting exchange terms, the third-order energy diagrams which involve only two hole states (one pair) are shown in Fig. 5. The hole-hole interaction is shown in Fig. 5(a) and hole-particle interactions in 5(b) and 5(c). The diagrams of Figs. 5(b) and 5(c) represent the net effect of the interactions of particles in excited states i and j with the passive unexcited states and with the potential V .⁵ It is assumed that i is calculated in the presence of all unexcited states except for q and j in the presence of all but r . In the case of open-shell atoms, there are still small corrections for each hole and particle line due to insertions of the type shown in Fig. 3. However, these were found to be very small (approximately 1%) in the calculations of this paper but they were included in most cases. The particle-particle (ladder) interaction is shown in Fig. 5(d). The diagrams of Figs. 5(a), 5(b), and 5(c) are exclusion-principle-violating (EPV) diagrams.⁵ It is also possible to have diagrams such as 5(a), 5(b), and 5(c) where the hole lines have different labels. These are less important, however, because in general the nondiagonal matrix elements are much smaller than the diagonal ones. When the excited states i , j , k , and l of Fig. 5 are bound states, the largest contributions for Fig. 5(b) come when $i=k$, for 5(c) when $j=l$, and for 5(d) when $i=k$ and $j=l$. In this diagonal case, these four third-order diagrams sum to give the second-order diagrams (with q , r excited into i , j) times the factor

$$(\epsilon_q + \epsilon_r - \epsilon_i - \epsilon_j)^{-1} \times (\langle qr|v|qr\rangle - \langle ir|v|ir\rangle - \langle qj|v|qj\rangle + \langle ij|v|ij\rangle). \quad (41)$$

This same factor is repeated in the higher orders, and this geometric series is summed to give the modified second-order result

$$D^{-1} |\langle ij|v|qr\rangle|^2, \quad (42)$$

where

$$D = (\epsilon_q + \epsilon_r - \langle qr|v|qr\rangle) - (\epsilon_i + \epsilon_j - \langle ir|v|ir\rangle - \langle qj|v|qj\rangle + \langle ij|v|ij\rangle). \quad (43)$$

The corresponding exchange matrix elements are also included when states q and r have parallel spins. The first term of D is the two-particle energy of electrons in states q and r , and the second term represents the two-particle energy for particles in states i and j .⁶ An analysis of higher order terms leads to the addition into Eq. (43) of terms $E_{\text{corr}}(q,n)$ and $E_{\text{corr}}(n \neq q, r)$, where $E_{\text{corr}}(q,n)$ is the correlation energy of q with all other un-

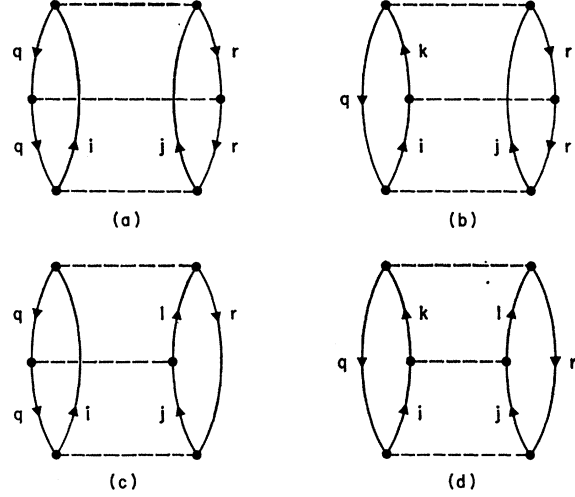


FIG. 5. Third-order energy diagrams involving only one electron pair. (a) Hole-hole interaction. (b) and (c) are hole-particle interactions which represent the net effect of interactions of particles in states i and j with the passive unexcited states and with the potential V . It is assumed that i is calculated in the field of all unexcited states except q and j in the field of all but r . (d) Particle-particle interaction or ladder diagram.

excited states and $E_{\text{corr}}(n \neq q, r)$ is the correlation energy of r with all other unexcited states except for q . These quantities are unknown at the outset and their effects on Eq. (43) may be calculated as a small correction when the main part of the calculation is finished.

When the excited states i and j are in the continuum, the geometric sum can be carried out only for the hole-hole interactions of Fig. 5(a), and D becomes

$$D = \epsilon_q + \epsilon_r - \langle qr|v|qr\rangle - \epsilon_i - \epsilon_j. \quad (44)$$

When the spins of q and r are parallel, we also add the exchange term $\langle qr|v|rq\rangle$ to Eq. (44). However, as shown in Ref. 5, the hole-particle interactions of Fig. 5(b) and higher orders may be included to good accuracy by calculating

$$a(k, k'; r) = \left(-\frac{2}{\pi} \int_0^\infty dk'' \langle kr|v|k''r\rangle D^{-1}(k'', k') \times \langle k''k'|v|qr\rangle \right) / \langle kk'|v|qr\rangle, \quad (45)$$

where

$$D(k''k') = \epsilon_q + \epsilon_r - \langle qr|v|qr\rangle - \frac{1}{2}k''^2 - \frac{1}{2}k'^2. \quad (46)$$

The value of k is a representative value from the range of k values which contribute most to the second-order integration. In Ref. 5, $a(k, k'; r)$ was found to be a slowly varying function of k and k' . To a good approximation $a(k, k'; r)$ is the ratio of the third-order diagram of Fig. 5(b) to the corresponding second-order diagram. The factor $a(k, k'; q)$ may be calculated to account for the diagram of Fig. 5(c). The corresponding approximation

TABLE III. $2p$ - $2p$ correlations in a.u. from continuum states.

Excitations ^a	Modified 2nd-order direct ^b	Modified 2nd-order exchange ^b	Modified 2nd-order total	Total including higher orders ^c
$2p(-1^+) \rightarrow ks^+$				
$2p(+1^-) \rightarrow k's^-$	-0.000579	0.0000	-0.000579	-0.000662
$2p^+ \rightarrow kp^+$				
$2p^+ \rightarrow k'p^+$	-0.01127	+0.00659	-0.01068	-0.01270
$2p^+ \rightarrow kp^+$				
$2p^- \rightarrow k'p^-$	-0.01860	0.0000	-0.01860	-0.02212
$2p^+ \rightarrow kd^+$				
$2p^+ \rightarrow k'd^+$	-0.01944	+0.00583	-0.01360	-0.01534
$2p^+ \rightarrow kd^+$				
$2p^- \rightarrow k'd^-$	-0.01930	0.0000	-0.01930	-0.02176
$2p^+ \rightarrow kf^+$				
$2p^+ \rightarrow k'f^+$	-0.00306	+0.00155	-0.00151	-0.00151 ^d
$2p^+ \rightarrow kf^+$				
$2p^- \rightarrow k'f^-$	-0.00316	0.00000	-0.00316	-0.00316 ^d
$2p^+ \rightarrow k^+s, kd^+$				
$2p^+ \rightarrow k'd^+, k's^+$	-0.00328	+0.00328	0.00000	0.00000
$2p^+ \rightarrow ks^+, kd^+$				
$2p^- \rightarrow k'd^-, k's^-$	-0.00468	0.00000	-0.00468	-0.00468 ^d
$2p^+ \rightarrow kp^+$				
$2p(+1^-) \rightarrow 2p(0^-, -1^-)$	-0.000761	0.0000	-0.000761	-0.000761
Total	-0.090131	+0.01725	-0.072871	-0.082691 ^e

^a k and k' refer to continuum excitations. s, p, d, f refer to $l=0, 1, 2, 3$.

^b Second order calculated with the modified D of Eq. (44).

^c Includes sum of hole-particle and ladder terms by Eq. (48).

^d Effects of higher order terms were estimated to be small and are not included.

^e This total is reduced by the contribution +0.00201 a.u. from the third-order ladder diagrams in which the $l=1$ continuum excitations scatter into $l=2$ excitations and also $l=2$ scattering into $l=1$ states. The new total is then -0.08068 a.u.

for the diagram of Fig. 5(d) is

$$t(k, k') = \left[\left(\frac{2}{\pi} \right)^2 \int_0^\infty dk'' \int_0^\infty dk''' \langle k k' | v | k'' k''' \rangle \right. \\ \left. \times D(k'', k''')^{-1} \langle k'' k''' | v | q r \rangle \right] / \langle k k' | v | q r \rangle, \quad (47)$$

where k, k' are again chosen to be typical excitations of importance in the second-order calculation. The factor $t(k, k')$ represents the ratio of the diagram of Fig. 5(d) to the second-order diagram with the same hole lines. It is assumed in Eqs. (45) and (47) that a and t also depend on l and l' of k and k' . As shown previously,⁵ the interactions shown in Figs. 5(b), 5(c), and 5(d) are repeated in higher orders and, to a good approximation, they may be summed geometrically to give the factor

$$[1 - a(k, k'; r) - a(k, k'; q) - t(k, k')]^{-1}, \quad (48)$$

which multiplies the second-order diagram with hole lines q and r and D given by Eq. (44). In Ref. 5 these effects were found to be much more important than in the present calculation owing to the fact that there were four a 's in the factor corresponding to Eq. (48) because of the choice of the potential V_{HF} . In addition, a and t in this calculation are approximately 0.15 and -0.15 for $2s$ and $2p$ hole lines as compared with 0.29 and -0.36 previously.⁵ Typically, the factor of Eq. (48) is between 1.00 and 0.85^{-1} in this calculation and an

error of 10% in a and t , which seems unlikely, would lead to errors of only 1 or 2% in Eq. (48).

C. Numerical Results

The results of the calculations for correlations among $2p$ electrons are given in Table III for excitations involving either two continuum excitations or one $2p$ excited state and one continuum excited state. The remaining $2p$ - $2p$ contributions from excitations into bound excited states with $n \geq 3$ are given in Table IV. In general, the excitations into bound states are much

TABLE IV. $2p$ - $2p$ correlation energies in a.u. from excitations into bound states with $n \geq 3$.

Excitation	Correlation energy
$2p^+ \rightarrow ms^+$	
$2p^\pm \rightarrow ns^\pm$	-0.000053
$2p^+ \rightarrow mp^+$	
$2p^\pm \rightarrow np^\pm$	-0.000791
$2p^+ \rightarrow mp^+$	
$2p(+1^-) \rightarrow 2p(0^-, -1^-)$	-0.000339
$2p^+ \rightarrow md^+$	
$2p^\pm \rightarrow nd^\pm$	-0.000003
$2p^+ \rightarrow kp^+, mp^+$	
$2p^\pm \rightarrow mp^\pm, kp^\pm$	-0.00795
$2p^\pm \rightarrow ns^\pm, kd^\pm$	
$2p^\pm \rightarrow kd^\pm, ns^\pm$	-0.000384
$2p^+ \rightarrow nd^+, kd^+$	
$2p^\pm \rightarrow kd^\pm, nd^\pm$	-0.000376
Total	-0.009896

TABLE V. Factors to sum hole-particle and ladder effects by Eq. (48).

Excitation	$a(k, k'; 2p)^a$	$t(k, k')^b$
$l=0$	0.125	-0.125
$l=1$	0.1630	-0.1669
$l=2$	0.1214	-0.1297

^a See Eq. (45). k and k' were chosen between 1.0 and 2.0 which is where the matrix elements $\langle kk'|v|2p2p\rangle$ were largest.

^b See Eq. (47).

less important than the excitations into continuum states. Although the energy denominators are smaller for bound-state excitations than for continuum excitations, the matrix elements connecting bound excited states with the $2p$ states are much smaller than for the continuum matrix elements due to the fact that the bound excited states are mostly at a much greater radial distance from the nucleus than the $2p$ states. The integrations were carried out from $k, k'=0.0$ to 20.0 , where the matrix elements were extremely small. The most important range for k was from 0.0 to 3.0 . The higher order terms were included by the factor of Eq. (48). The values for a and t for different l excitations are given in Table V. For example, for $a(k, k', 2p)$ the value $k=k'=1.50$ was used for $l=1$.

The value for the total correlation energy among $2p$ electron pairs from Tables III and IV is -0.09259 a.u. However, this values does not include the effects of third-order ladder diagrams in which excited states interact and scatter from excited states of given l values to excited states with different orbital momentum l . The contribution from these diagrams in which excited states $kp, k'p$ scatter into $kd, k'd$ and diagrams in which $kd, k'd$ scatter into $kp, k'p$ was calculated to be $+0.00201$ a.u. This gives a new total of -0.09058 a.u. The calculations of Table III also include effects of insertions on the hole lines and particle lines as shown for hole lines in Fig. 3. These were found to be very small, approximately 1% effects. Since a restricted HF basis is used there are also energy terms of the type shown in Figs. 4(c), 4(d), and 4(e), and also the same types of diagrams with potential interactions. The total of these terms for $2p$ electrons excited into kp states was found to be -0.00113 a.u. This small value shows that for $2p$ electrons the use of a restricted HF potential rather

TABLE VI. Comparison of second-order correlation energies and accurate values.^a

Excitations	Second order	Modified second order ^b	Accurate value ^c
$2p^+ \rightarrow kp^+$			
$2p^\pm \rightarrow k'p^\pm$	-0.03576	-0.02928	-0.03482
$2p^+ \rightarrow kd^+$			
$2p^\pm \rightarrow k'd^\pm$	-0.03799	-0.03290	-0.03710

^a All energies are in a.u.

^b Calculated with modified denominator of Eq. (46); only includes higher order terms due to hole-hole interactions.

^c Taken from Table III.

TABLE VII. Effect of R_0 on matrix elements.^a

k	$\langle 2p2.0d v 2pkd\rangle(R_0=50.0)$	$\langle 2p2.0d v 2pkd\rangle(R_0=30.0)$
0.50	0.041918	0.025130
1.00	0.132219	0.124473
1.25	0.233244	0.242012
1.50	0.400139	0.440386
1.625	0.528058	0.488384
1.75	0.714685	0.782329
1.875	1.037463	1.012214
2.00	2.232088	1.978391
2.125	1.051450	1.029288
2.25	0.739979	0.800411
2.375	0.563280	0.530494
2.50	0.444062	0.473694
2.75	0.290690	0.291278
3.00	0.197229	0.189353
3.50	0.095408	0.105623
4.00	0.047407	0.051722
5.00	0.011232	0.018026
6.00	0.001395	0.005200
8.00	-0.001646	-0.000664
10.00	-0.001066	0.000212
12.00	-0.000455	-0.000777

^a All continuum states of this table have $l=2$.

than an unrestricted HF potential has an almost negligibly small effect on the correlation energy when compared with the true two-body correlations of Tables III and IV. Adding the value -0.00113 a.u. to the previous total, we find that the total correlation energy among $2p$ electrons is now -0.09171 a.u.

This result is close to what is obtained by calculating true second-order terms only. A comparison between some of the true second-order terms, second-order terms with the modified denominators of Eq. (46), and the correct pair correlations is given in Table VI. For $2p$ electrons, the second-order result is only a few percent higher than the value we obtain by a careful consideration of higher order terms. The reason that this second-order value is better than that obtained with the shifted

TABLE VIII. $2s$ - $2p$ correlation energies in a.u. from excitations involving $2p$ excited states.

Excitations ^a	Second-order direct ^b	Second-order exchange ^b	Total
$2s^- \rightarrow 2p(0^-, -1^-)$			
$2p^\pm \rightarrow kd^\pm$	-0.04301	0.00626	-0.03675
$2s^\pm \rightarrow kd^\pm$			
$2p(+1^-) \rightarrow 2p(0^-, -1^-)$	-0.005589	0.00626	0.000671
$2s^- \rightarrow 2p(0^-, -1^-)$			
$2p(0^+, -1^+) \rightarrow ks^+$	-0.000796	0.00000	-0.000796
$2s^- \rightarrow 2p(0^-, -1^-)$			
$2p^\pm \rightarrow ns^\pm$	-0.000388	0.00000	-0.000388
$2s^- \rightarrow 2p(0^-, -1^-)$			
$2p^\pm \rightarrow nd^\pm$	-0.000270	0.000037	-0.000233
$2s^\pm \rightarrow ns^\pm$			
$2p(+1^-) \rightarrow 2p(0^-, -1^-)$	-0.000020	0.000037	0.000017
Total	-0.05007	0.01259	-0.03748

^a k refers to continuum excitations and n, m refer to bound states. $m, n \geq 3$.

^b The terms involving one continuum excited state and one bound excited state were calculated with the denominator of Eq. (49) to account for one of the hole-particle interactions and the hole-hole interaction.

TABLE IX. $2s$ - $2p$ correlation energies in a.u. from two-continuum excitations.

Excitations	Modified 2nd-order direct ^a	Modified 2nd-order exchange ^a	Modified 2nd-order total	Total including higher orders ^b
$2s \rightarrow ks$				
$2p \rightarrow k'p$	-0.02785	+0.004898	-0.02295	-0.02623
$2s \rightarrow kp$				
$2p \rightarrow k's$	-0.004100	+0.004898	+0.0007980	+0.000912
$2s \rightarrow kp$				
$2p \rightarrow k'd$	-0.012917	+0.003320	-0.009597	-0.01097
$2s \rightarrow kd$				
$2p \rightarrow k'p$	-0.003640	+0.003320	-0.000320	-0.000366
$2s \rightarrow kd$				
$2p \rightarrow k'f$	-0.01589		-0.01589	-0.01589
Total	-0.064397	+0.016436	-0.047959	-0.05254

^a Calculated with the modified denominator D of Eq. (44).

^b Includes sum of higher order terms by Eq. (48).

D of Eq. (46) is that with the basis set of this calculation there are two hole-particle diagrams in third order which increase the second-order result, whereas the hole-hole and particle-particle diagrams reduce the second-order term. These terms are often of comparable size and tend to cancel. When only one of them is included [for example, by D of Eq. (46)], there is in effect an unbalance, and the rough cancellation in higher orders does not occur. In the calculations of Ref. 5 the HF basis was used and in this case there are four hole-particle diagrams in third order and so the rough cancellation does not take place.

In calculating matrix elements for second-order energy terms it is only necessary to carry out the radial integrals to the radius where the unexcited-state wave functions are effectively zero. However, in higher orders we encounter matrix elements with continuum to continuum transitions. There is no natural cutoff now on

TABLE X. $2s$ - $2p$ correlation energies in a.u. from excitations involving bound states other than $2p$.

Excitations ^a	Second-order direct	Second-order exchange	Second-order Total
$2s \rightarrow ns$			
$2p \rightarrow kp$	-0.006845	0.00104	-0.005805
$2s \rightarrow kp$			
$2p \rightarrow ns$	-0.0006290	0.00104	0.00041
$2s \rightarrow ks$			
$2p \rightarrow np$	-0.003210	0.000474	-0.002736
$2s \rightarrow np$			
$2p \rightarrow ks$	-0.000279	0.000474	0.000195
$2s \rightarrow np$			
$2p \rightarrow kd$	-0.002173	0.000495	-0.001678
$2s \rightarrow kd$			
$2p \rightarrow np$	-0.000466	0.000495	0.000029
$2s \rightarrow ms$			
$2p \rightarrow np$	-0.001020	0.000150	-0.000870
$2s \rightarrow mp$			
$2p \rightarrow ns$	-0.000110	0.00015	0.000040
$2s \rightarrow mp$			
$2p \rightarrow nd$	-0.000001	0.000000	-0.000001
Total	-0.014733	0.004318	-0.030416

^a $n, m \geq 3$.

the radial integrations, and we must decide on a physical R_0 . We expect that R_0 can have any value which is much larger than the "radius" of the atom. Physically, we should not expect the structure of the atom to depend on the size of its container provided this containing volume is very large compared to the atom. In the present calculations R_0 was chosen as 50.0 as compared with the maximum orbital density of the oxygen atom which occurs at 0.85 according to the HF calculations.¹³ Although the matrix elements for continuum to continuum transitions still depend on R_0 , in calculating the energy or other physical quantities we integrate over the intermediate continuum states and the result then does not depend on R_0 . An example of this effect is shown in Table VII where the matrix elements are sensitive to R_0 . However, when the quantity $a(2.0, 2.0; 2p)$ of Eq. (45) was calculated for $l=2$ states, the result was 0.121 using $R_0=50.0$ and 0.119 using $R_0=30.0$.

The results for $2s$ - $2p$ correlations are given in Tables VIII, IX, and X. It is seen that the bound-state excitations of greatest importance are $2s^- \rightarrow 2p(0^-, -1^-)$. In calculating the contributions of Table VIII, when the $2s$ electron is excited into a $2p$ excited state and the other excited state is in the continuum,

$$D = \epsilon_{2s} + \epsilon_{2p} - \langle 2s2p | v | 2s2p \rangle - (\epsilon_{2p} + \frac{1}{2}k^2 - \langle 2s2p | v | 2s2p \rangle). \quad (49)$$

We have accounted for one of the two hole-particle interactions by including $\langle 2s2p | v | 2s2p \rangle$ in D , which is

TABLE XI. $2s$ - $2s$ correlation energies in a.u.

Excitations ^a	Modified second-order result ^b	Total ^c
$2s^+ \rightarrow ks^+$		
$2s^- \rightarrow k's^-$	-0.00250	-0.00286
$2s^+ \rightarrow kp^+$		
$2s^- \rightarrow k'p^-$	-0.00162	-0.00185
$2s^+ \rightarrow kd^+$		
$2s^- \rightarrow k'd^-$	-0.00463	-0.00529
$2s^+ \rightarrow kf^+$		
$2s^- \rightarrow k'f^-$	-0.00135	-0.00135
$2s^+ \rightarrow kp^+$		
$2s^- \rightarrow 2p(0^-, -1^-)$	-0.00184	-0.00184
$2s^+ \rightarrow np^+$		
$2s^- \rightarrow 2p(0^-, -1^-)$	-0.000595	-0.000595
$2s^+ \rightarrow ns^+, ks^+$		
$2s^- \rightarrow ks^-, ns^-$	-0.000804	-0.000804
$2s^+ \rightarrow np^+, kp^+$		
$2s^- \rightarrow k'p^-, np^-$	-0.000274	-0.000274
$2s^+ \rightarrow ms^+$		
$2s^- \rightarrow ns^-$	-0.000118	-0.000118
$2s^+ \rightarrow mp^+$		
$2s^- \rightarrow np^-$	-0.000020	-0.000020
$2s^+ \rightarrow md^+$		
$2s^- \rightarrow nd^-$	-0.0000001	-0.0000001
Total	-0.01375	-0.01500

^a k and k' refer to continuum states and n, m to bound excited states with $n, m \geq 3$.

^b Shifted denominator of Eq. (49) is used when there is one bound and one continuum excited state. D of Eq. (44) is used for k, k' excitations.

^c Higher order effects of Eq. (48) are included for all k, k' excitations except for $k', k'f$.

TABLE XII. $1s$ - $2p$ correlation energies in a.u.

Excitations ^a	Modified second-order direct ^b	Modified second-order exchange ^b	Modified second-order total ^b	Total ^c
$1s \rightarrow ks$				
$2p \rightarrow k'p$	-0.001391	-0.000537	-0.001927	-0.002079
$1s \rightarrow kp$				
$2p \rightarrow k's$	-0.001326	-0.000537	-0.001863	-0.002009
$1s \rightarrow kp$				
$2p \rightarrow k'd$	-0.009349	0.001110	-0.008239	-0.008888
$1s \rightarrow kd$				
$2p \rightarrow k'p$	-0.001014	0.001110	0.000096	0.000104
$1s \rightarrow kd$				
$2p \rightarrow k'f$	-0.001376	0.0003120	-0.001064	-0.001148
$1s \rightarrow kf$				
$2p \rightarrow k'd$	-0.000389	0.000312	-0.000077	-0.000083
$1s^- \rightarrow 2p(0^-, -1^-)$				
$2p \rightarrow kd$	-0.000648	0.000090	-0.000558	-0.000558
$1s \rightarrow kd^\pm$				
$2p(+1^-) \rightarrow 2p(0^-, -1^-)$	-0.000104	0.000090	-0.000014	-0.000014
$1s^- \rightarrow 2p(0^-, -1^-)$				
$2p(0^+, -1^+) \rightarrow ns^+$	-0.000005	0.000000	-0.000005	-0.000005
$1s \rightarrow ns$				
$2p \rightarrow kp$	-0.000036	-0.000022	-0.000058	-0.000058
$1s \rightarrow kp$				
$2p \rightarrow ns$	-0.000062	-0.000022	-0.000084	-0.000084
$1s^- \rightarrow 2p(0^-, -1^-)$				
$2p(0^+, -1^+) \rightarrow ks$	-0.000063	0.000000	-0.000063	-0.000063
$1s \rightarrow np$				
$2p \rightarrow ks$	-0.000015	-0.000004	-0.000019	-0.000019
$1s \rightarrow ks$				
$2p \rightarrow np$	-0.000005	-0.000004	-0.000009	-0.000009
$1s \rightarrow np$				
$2p \rightarrow kd$	-0.000104	0.000021	-0.000083	-0.000083
Total	-0.015887	0.001919	-0.013967	-0.014996

^a k, k' are continuum states. m, n refer to bound states with $m, n \geq 3$.

^b D of Eq. (44) used for k, k' excitations.

^c k, k' excitation terms are modified by Eq. (48).

now the second-order denominator. The remaining hole-particle interaction and the particle-particle interaction are expected to cancel to a good approximation as they did in the $2p$ - $2p$ case as seen in Table V and so the second-order result is taken as the pair correlation energy. The total $2s$ - $2p$ correlation energy from Tables VIII, IX, and X is -0.1004 a.u.

The correlation energies for different excitations for the $2s$ - $2s$ pair are given in Table XI. In the case of $2s^- \rightarrow 2p(0^-, -1^-)$ excitations, one hole-particle interaction is included by adding $\langle 2s2p | v | 2s2p \rangle$ to D of Eq. (44). In the two-continuum excitation cases, the hole-particle and ladder interactions were included by the factor of Eq. (48). Small effects for the insertions of Fig. 3 were also included. The excitations into bound $l=2$ states were extremely small. The total $2s$ - $2s$ correlation energy of -0.01500 a.u. is considerably smaller than the $2s$ - $2s$ beryllium correlation energy of -0.04491 a.u.^{5,6} This relatively small $2s$ - $2s$ correlation energy in oxygen may be ascribed to the exclusion principle as discussed previously by McKoy and Sinanoğlu.¹⁷ If the presence of the four oxygen $2p$ electrons is ignored, then

there is a contribution of -0.0607 a.u. in second order to the $2s$ - $2s$ correlation energy due to excitations into the $2p$ excited states. However, the exclusion principle must be considered and so this contribution may not be included.

There is also the small contribution to the correlation energy due to the diagrams of Figs. 4(c), 4(d), and 4(e) because the potential we use is not a completely unrestricted HF potential. The potential of Eq. (26) has two $2p$ exchange interactions for both $2s^\pm$ states, but the $2s^+$ electron actually has exchange interactions with the three $2p^+$ electrons and the $2s^-$ has exchange interactions with the one $2p^-$ electron. This effect causes the diagram of Fig. 4(d) to be included for both $2s^\pm$, with excitations into ks^\pm states giving a total of -0.000769 a.u. There is also an energy of -0.000814 a.u. from diagrams shown in Figs. 4(c), 4(d), and 4(e) in which $2s^\pm$ electrons are excited into kd^\pm states. The total $2s$ - $2s$ correlation energy, referred to the restricted HF solution, is then -0.01661 a.u.

The remaining contributions to the correlation energy come from $1s$ - $1s$ correlations and from the $1s$ - $2s$ and $1s$ - $2p$ intershell correlations. The $1s$ - $2p$ correlations are given in Table XII and give a total $1s$ - $2p$ correlation energy of

¹⁷ V. McKoy and O. Sinanoğlu, J. Chem. Phys. 41, 2689 (1964).

TABLE XIII. 1s-2s correlation energies in a.u.

Excitations ^a	Modified second-order direct ^b	Modified second-order exchange ^b	Modified second-order total ^b	Total ^c
1s → ks				
2s → k's	-0.003160	0.001537	-0.001623	-0.001688
1s → kp				
2s → k'p	-0.003910	0.001189	-0.002721	-0.002830
1s → kd				
2s → k'd	-0.000940	0.000329	-0.000611	-0.000635
1s → kf				
2s → k'f	-0.000248	0.000101	-0.000147	-0.000153
1s [±] → kp [±]				
2s ⁻ → 2p(0 ⁻ , -1 ⁻)	-0.000799	0.000046	-0.000753	-0.000753
1s ⁻ → 2p(0 ⁻ , -1 ⁻)				
2s ⁺ → kp	-0.000136	0.000046	-0.000090	-0.000090
1s → np				
2s → kp	-0.0000241	0.000006	-0.000018	-0.000018
1s → kp				
2s → np	-0.000089	0.000006	-0.000083	-0.000083
1s → ks				
2s → ns	-0.000020	0.000013	-0.000007	-0.000007
1s → ns				
2s → ks	-0.000036	0.000013	-0.000023	-0.000023
1s ⁻ → 2p(0 ⁻ , -1 ⁻)				
2s [±] → np	-0.000009	0.000006	-0.000003	-0.000003
1s [±] → np [±]				
2s ⁻ → 2p(0 ⁻ , -1 ⁻)	-0.000014	0.000006	-0.000008	-0.000008
Total	-0.009385	0.003298	-0.006087	-0.006291

^a k, k' are continuum excitations. m, n refer to bound states with $m, n \geq 3$.

^b D of Eq. (44) has been used.

^c Hole-particle and particle-particle effects are included by Eq. (48) for k, k' excitations. The second-order result is used for bound excited states.

-0.014996 a.u. The total 1s-2p correlation energy, although small compared to 2p-2p and 2s-2p correlations, is still sufficiently large that it must be included if an accurate value for the total correlation energy is desired. The 1s-2s intershell correlation energy is given in Table XIII and is -0.006291 a.u. The average correlation energy for each 1s-2s pair is -0.00157 a.u. as compared with an average correlation energy -0.00187 a.u. for each 1s-2p pair. The average effect of the hole-particle and particle-particle interactions for 1s-2s correlations is to multiply the modified second-order terms involving two-continuum excitations by approximately 1.04. The 1s-1s correlation energy contributions listed in Table XIV add to give a total of -0.04383 a.u.

Since the excited single-particle states in this investigation are calculated in the presence of both 1s electrons, when there is a 1s hole line both excited states interact with it. That is, the interactions of the excited states with V and with the unexcited states do not completely cancel and give rise to these hole-particle interactions. There may also be interactions with a 2s or 2p state which was omitted in V but is now present. For example, consider 1s-2p correlations into $kp, k'd$ states. There are hole-particle interactions of both kp and $k'd$ with the 1s hole line because kp and $k'd$ are calculated with V in which both 1s electrons are present and one 2p electron is removed. There will be no hole-particle interactions with the 2p hole line in this case. It should be

noted that in general there will be small effects due to insertions on hole and particle lines of the type shown in Figs. 3(b), 3(c), and 3(d). The hole-particle interactions merely account for the major effects of the lack of cancellation between interactions with V and with the passive unexcited states.

For the 1s-1s correlations both excited states interact with each 1s hole line giving a total of four hole-

TABLE XIV. 1s-1s correlation energies in a.u.

Excitations ^a	Modified second-order total ^b	Total ^c
1s ⁺ → ks ⁺		
1s ⁻ → k's ⁻	-0.011788	-0.013173
1s ⁺ → kp ⁺		
1s ⁻ → k'p ⁻	-0.021848	-0.024413
1s ⁺ → kd ⁺		
1s ⁻ → k'd ⁻	-0.003716	-0.004152
1s ⁺ → kf ⁺		
1s ⁻ → k'f ⁻	-0.001063	-0.001188
1s ⁺ → kp ⁺		
1s ⁻ → 2p(0 ⁻ , -1 ⁻)	-0.000634	-0.000634
1s ⁺ → kp ⁺ , np ⁺		
1s ⁻ → np ⁻ , kp ⁻	-0.000117	-0.000117
1s ⁺ → ks ⁺ , ns ⁺		
1s ⁻ → ns ⁻ , ks ⁻	-0.000152	-0.000152
Total	-0.039318	-0.043829

^a k, k' refer to continuum states. m, n refer to bound states with $m, n \geq 3$.

^b States with k, k' calculated with D of Eq. (44).

^c Includes hole-particle and particle-particle effects by Eq. (50) for k, k' excitations.

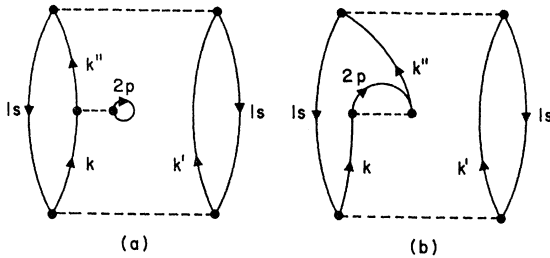


FIG. 6. Third-order diagrams which should be included in $1s$ - $1s$ correlated in a potential V which omits one $2p$ state. For $l=0$ states, $2p$ is replaced by $2s$. (a) Direct interaction. (b) Corresponding exchange term.

particle interactions rather than two as given by Eq. (48). These terms are partly cancelled by the particle-particle interactions and by the interactions of excited states with a $2p$ or $2s$ state excluded from V but now present. This type of term is shown in Fig. 6. These terms are included by the methods used in Eq. (48). However, the appropriate factor is now

$$[1 - 4a(k, k'; 1s) - t(k, k') + 2a(k, k'; 2p)]^{-1}, \quad (50)$$

where a and t are defined by Eqs. (45) and (47). The term $a(k, k'; 2p)$ in Eq. (50) should account for the exchange term of Fig. 6(b) as well as for the direct term of Fig. 6(a). In the case of $k\bar{p}, k'\bar{p}$ excitations, $t(k, k')$ was found to be approximately equal to $-a(k, k'; 1s)$. The term $a(k, k'; 1s)$ was calculated to be 0.0431 and $a(k, k'; 2p)$ was 0.0121. For $k\bar{p}, k'\bar{p}$ excitations of two $1s$ electrons, Eq. (50) is then 1.1174.

As discussed previously, the $1s$ states were calculated with interactions with only one $2s$ electron of opposite spin and with interactions with one $1s$ electron of parallel spin and one of antiparallel spin. Each $1s$ electron interacts, however, with a $2s$ electron of parallel spin and one of antiparallel spin and with only one $1s$ electron of opposite spin. The interaction of a $1s$ electron with a $1s$ electron of parallel spin in V may be neglected since the exchange $1s$ interaction cancels the direct term. The net effect is that diagrams of Fig. 2(a) and 2(b) must be calculated for $p=1s^+$ and $n=2s^+$ and for $p=1s^-$ and $n=2s^-$. The corresponding energy diagrams are shown in Figs. 4(c), 4(d), and 4(e). The diagrams of Fig. 4(c) were found to give -0.0001322 a.u. and those of Fig. 4(d) gave -0.0002522 a.u. The diagrams of Fig. 4(e) gave 0.0003629 a.u., making a total -0.0000215 a.u. This value should not be included in the correlation energy, however, as it is the difference between the restricted HF energy and the energy through first order using the potential of Eq. (26) for both $1s$ and $2s$ states.

As in the case of $2s$ electrons, there are also corrections of the type shown in Fig. 4(d) with $q=1s^\pm$ and $n=2p^\pm$ due to the fact that a restricted HF potential is used. The sum of diagrams like Fig. 4(d) for $1s^\pm$ excitations into $k\bar{s}$ states was calculated to be -0.0000632 a.u. and -0.0000223 a.u. for excitations into $k\bar{d}$ states. These

values are included in the correlation energy which is referred to the restricted HF solution. The total $1s$ correlation energy is then -0.04392 a.u.

D. Discussion of Results

The results of the correlation energy calculations are summarized in Table XV. The total correlation energy -0.2740 a.u. is composed both of true two-body correlations which equal -0.2711 a.u. and of one-body effects equal to -0.00283 a.u. These one-body effects, as discussed previously, are due to the use of a spherically symmetric, restricted HF potential rather than a completely unrestricted HF potential. The value -0.2740 a.u. is 5.84% more negative than the value -0.258 a.u. which Clementi has deduced from experiment as the total oxygen correlation energy and which he estimates as accurate to within 5%. The difference between the results of the present calculation and the correct total correlation energy may be attributed both to the approximations in calculating the pair correlations and also to the neglect of three-body and higher effects. If we neglect the possible errors in Clementi's value for E_{corr} and in the value from this investigation, the difference 0.016 a.u. gives us a very rough estimate of the size of the three-body and higher correlation effects in neutral oxygen. Since this value is quite inaccurate and could even be wrong in sign, it would be desirable to calculate three-body effects directly.

The calculations of this paper for one-body and two-body correlations are estimated as being accurate to within approximately 5%. Most of this inaccuracy is attributed to the neglect of nondiagonal ladder diagrams and omission of excited states with $l > 3$. The individual contributions listed in the tables are estimated to be accurate to within 2%. The nondiagonal ladder diagrams which are expected to be largest for $2p$ - $2p$ correlations have been included. These are the diagrams in which two $2p$ electrons, excited into $l=1$ states, scatter into $l=2$ states before returning to the ground state and those diagrams in which particles in $l=2$ states scatter into $l=1$ excited states before returning to the ground state. These terms contributed 0.00201 a.u. No other

TABLE XV. Summary of contributions to the correlation energy in a.u.^a

Electrons	Correlation energy
$ 2p-2p$	-0.09058
$2s-2p$	-0.10044
$ 2s-2s $	-0.01500
$ 1s-2p$	-0.014996
$1s-2s$	-0.00629
$1s-1s$	-0.04383
$2p^b$	-0.00113
$2s^b$	-0.00161
$1s^b$	-0.000086
Total	-0.2740

^a Only one-body and two-body contributions are included.

^b One-body corrections due to use of a restricted Hartree-Fock potential

nondiagonal ladder terms have been included. For the correlations involving at least one $1s$ electron, the non-diagonal ladder diagrams are very small due to the large energy denominators. Omission of the ladder diagrams tends to make the correlation energy more negative and omission of states with $l > 3$ causes the correlation energy to be less negative.

From Tables III, IV, VIII, IX, and XII it is found that the correlation energy terms involving the $2p(+1^-)$ state add to approximately -0.079 a.u. This value may be compared with the difference in correlation energy between O and O^+ (-0.065 a.u.) or between O and N (-0.070 a.u.).¹⁵ Actually, an adjustment should be made to account for the fact that since the state $2p(+1^-)$ is unoccupied in O^+ and N, excitations into this state may occur and there is an approximate change in the correlation energy in O^+ and N by -0.0063 a.u. relative to that in O due to all electrons other than $2p(+1^-)$. This provides another example of the effects of the exclusion principle.

E. Three-Body Effects

An advantage of the perturbation expansion is that the three-body and higher terms enter in a systematic manner and are added directly to the one-body and two-body terms without repeating the part of the calculation for the pair correlations. The orthonormal set of states used to calculate the pair correlations is also used to calculate the three-body and higher diagrams. Three-body diagrams for the energy first enter in third order and they are shown in Figs. 7(a) and 7(b). The hole states q , r , and s must all be different for three-body terms. The most important contributions are expected when q , r , and s are $2s$ and $2p$ states. The diagrams of Fig. 7(a) are positive while the diagrams of Fig. 7(b) are negative. In Fig. 7(b) the spin of state q must be parallel to that of state r , while there is no such restriction in Fig. 7(a). Because of the angular factors in the matrix elements, the contributions from Fig. 7(b) are expected to be very small when q and r are $2p$ states. However, when q is a $2s$ state and r is a $2p$ state or q is a $2p$ state and r a $2s$ state, these diagrams will be significant. Although the diagrams of Figs. 7(a) and 7(b) have not been explicitly calculated, they are estimated as small compared with the pair correlations.

Some of the three-body diagrams in fourth order are shown in Figs. 7(c), 7(d), and 7(e). Diagrams like Fig. 7(c) have recently been included in studies of three-body correlations in nuclear matter.¹⁸ The diagrams of Figs. 7(d) and 7(e) are rearrangement diagrams of the type considered by Brueckner and Goldman.¹⁹ In Ref. 5 the diagrams of Fig. 7(d) were shown to arise from the linked cluster factorization and were called third-class EPV diagrams. In the diagrams of Fig. 7(d) the hole lines q

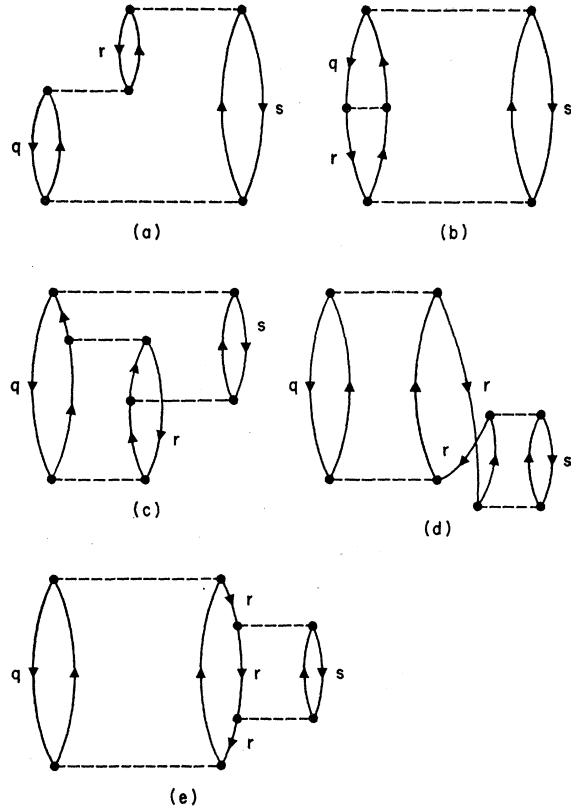


Fig. 7. Typical three-body diagrams. (a) Third-order "ring" diagram. (b) Exchange diagram of (a) or hole-particle diagram. (c) Fourth-order diagram of type considered in Ref. 18. (d) and (e) are rearrangement diagrams discussed in Ref. 19.

and s may be equal and in this case the diagram is no longer a three-body diagram but is part of the pair correlations. By considering both time orderings of the right-hand part of this diagram and the corresponding higher order diagrams, we may sum these diagrams in such a way that they may be included by a small shift in the denominator D of Eq. (43).²⁰ The rearrangement diagram of Fig. 7(e) also is an exclusion-principle-violating diagram resulting from the linked cluster factorization. Calculation of the diagrams gave approximately 0.0041 a.u. for Fig. 7(d) and -0.0045 a.u. for Fig. 7(e), so there is good cancellation between these two types of diagrams.

VI. DISCUSSION AND CONCLUSIONS

It has been shown in this investigation that many-body perturbation theory need not be restricted to closed-shell, nondegenerate systems but may be applied directly to calculation of the ground-state energy and wave function of most atoms. It was emphasized that it is important to start from an unperturbed eigenstate of L^2 , L_z , S^2 , and S_z . In calculating the single-particle

¹⁸ H. A. Bethe, Phys. Rev. 138, B804 (1965).

¹⁹ K. A. Brueckner and D. T. Goldman, Phys. Rev. 117, 207 (1960).

²⁰ H. P. Kelly, Phys. Rev. 134, A1450 (1964).

states it is important to use a potential which is spherically symmetric and independent of spin orientation. It was discussed why it is desirable in many-body perturbation calculations to choose the potential so that the single-particle excited states are calculated in the field of $N-1$ other electrons rather than in the field of N other electrons as is the case if the usual HF potential is used. The result in the present oxygen calculation is that the $2s$ and $2p$ states are HF orbitals but the $1s$ state differs slightly from the HF $1s$ solution. This difference caused $\langle \Phi_0 | H | \Phi_0 \rangle$ to be only 0.0000215 a.u. higher than the Hartree-Fock energy which is -74.80936 a.u. Bound and continuum excited states were calculated for $l=0, 1, 2,$ and 3 . The perturbation theory was then applied to the calculation of the correlation energy among all electrons of neutral oxygen. Sums over continuum states were carried out by numerical integrations and sums over the infinite set of bound states were carried out by the n^{-3} rule.⁶ The final result from calculation of the pair correlations and small one-body effects is that the total pair correlation energy is -0.2740 a.u. as compared with the correlation energy -0.258 a.u. deduced from experiment by Clementi.¹⁵ Most of the contributions to the correlation energy come from continuum states and from the excited $2p$ states of the unfilled $2p$ subshell. It is interesting that

the $2s-2p$ intershell correlation energy of -0.1004 a.u. is 37% of the total correlation energy. The total intershell correlation energy from $2s-2p$, $1s-2p$, and $1s-2s$ correlations is -0.1217 a.u. or 44% of the total correlation energy as compared with the previous beryllium calculation where the intershell energy was only 5% of the total. The importance of intershell effects may become even greater for larger atoms as the shells and subshells of electrons become closer.

The total pair correlation energy -0.2740 a.u. calculated in this work is estimated as being accurate to within 5% and Clementi also gives a limit of 5% on the accuracy of the value for the total correlation energy -0.258 a.u. deduced from experiment. Although the difference of 0.016 a.u. between the two correlation energy values may be due to three-body and higher correlations, the uncertainties in the two values make it desirable to carry out a direct calculation of three-body correlations and these effects will be investigated in future work.

ACKNOWLEDGMENTS

I would like to thank Professor Keith A. Brueckner for his support and encouragement and Dr. Katuro Sawada for helpful discussions.